<500ns Latency Overhead Analog-to-digital-compression Radio-over-fiber (ADX-RoF) Transport of 16-channel MIMO, 1024QAM Signals with 5G NR Bandwidth

Paikun Zhu[1], Yuki Yoshida[2], and Ken-ichi Kitayama[1,2]
1. The Graduate School for the Creation of New Photonics Industries (GPI), Hamamatsu, Shizuoka 431-1202, Japan
2. National Institute of Information and Communications Technology (NICT), Koganei, Tokyo 184-8795, Japan
zpk@gpi.ac.jp yuki@nict.go.jp kitayama@gpi.ac.jp

Abstract: Real-time analog-to-digital-compression radio-over-fiber (ADX-RoF) transport with <500ns processing latency overhead is demonstrated by using a single-chip programmable radio platform. 16-channel 61.44MHz 1024QAM-OFDM signals of 5G NR-class is delivered with ~4-Gb/s optical OOK interface, maintaining EVM<1.4%. © 2020 The Author(s)

1. Introduction

The development of next-generation radio access network (RAN) has attracted much attention in recent years, driven by the need of higher speed, higher connection density and lower end-to-end latency [1]. To deliver broadband wireless data from/to edge cloud to/from antenna sites that communicate with mobile terminals, wired-wireless convergence technology such as radio-over-fiber (RoF) is regarded as a promising candidate. Both digital RoF (D-RoF) [2-4] and analog RoF (A-RoF) [5-7] schemes have been actively discussed. In 5G and beyond, such schemes need to fulfill the requirements of: (a) Low latency overhead in addition to the essential fiber propagation delay; (b) High in-band fidelity with wide bandwidth, e.g., 1024QAM and 5G new radio (NR); (c) Scalability to multi-input-multi-output (MIMO) and even massive MIMO; (d) Low out-of-band emission for downlink; (e) Adaptivity against varied channel/power fading, bandwidth and wireless formats; (f) Compatibility to networking/switching. In this regard, traditional D-RoF (e.g., CPRI [2]) may not be practical due to huge optical bandwidth required. A-RoF is very spectrally efficient, but it is challenging to maintain high in-band signal quality and to support networking.

We suggest an alternative analog-to-digital-compression RoF (ADX-RoF) scheme to meet these requirements: MIMO waveforms are converted to "digital radio bearer" suitable for wired networking, meanwhile the data is compressed to save wired bandwidth and cost with limited signal distortion and low delay. Moreover, compression and optical channel coding/modulation are jointly optimized in this converged wired-wireless link [8]. the ADX-RoF can be viewed as an intermediate pathway between A-RoF and D-RoF: it can largely ease constraints of the fiber transmission owing to the bandwidth efficiency close to A-RoF, while radio signal fidelity can be higher than A-RoF due to the ADX DSP and the reliable digital optical format. We recently reported a preliminary ADX implementation [9]; yet its circuit throughput is only ≈5.5MHz, which would induce large buffering latency when handling large wireless bandwidth and/or heavy traffic load. High-throughput and low-latency are both indispensable towards a real-time, future-proof ADX-RoF system.

In this work, we present the first demonstration of ADX-RoF transport of 16-channel MIMO, 61.44MHz 5G NR-class signals with <500ns processing latency overhead, enabled by a real-time high-throughput ADX prototyped on a single-chip programmable radio platform. 32.4Gb/s CPRI-equivalent rate is delivered over 23.5km fiber using only ≈4-Gb/s optical OOK, with measured average EVM<1.4%.

2. Real-time ADX Design and Experimental Setup

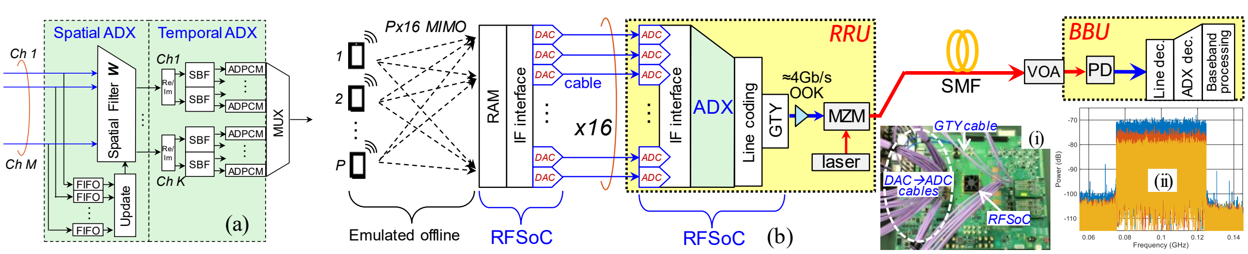

Fig. 1. (a) Designed real-time high-throughput ADX. ($K<M$) (b) Experimental setup. IF: intermediate frequency. RAM: random access memory. Inset (i): photo of RFSoC-based prototype; (ii): Measured spectra of 3 IF channels among 16.

An example ADX architecture may consist of spatial compression, temporal compression/quantization, optional spectrum efficiency (SE) enhancement of optical link (e.g., by multi-level PAM), and joint optimization [8, 9]. In [10], we proposed concepts of high-fidelity low-complexity spatial compression based on subspace tracking adaptive filter (e.g., PAST [11]) and temporal compression based on adaptive differential quantization (e.g., ADPCM [12]). However, the feedback loops in the concepts severely limits the circuit throughput to be much lower than the wireless bandwidth [9], which thus requires FIFO with buffering latency proportional to wireless packet size. In practice, high throughput is crucial for 5G NR-compliant real-time ADX. In this work, 2 main techniques for improving throughput are designed as shown in Fig. 1(a). For spatial ADX, we propose to decouple the forward filtering part and feedback filter update part. Spatial filter is updated every L wireless samples (L=10 in the implementation for 61.44MHz throughput). Since the filter update part converges rapidly (typically, $\approx 10^2 L$ samples or 17μs), variation of MIMO channel (ms-level) can be caught up even with such decoupling. In temporal ADX, we propose to use subbanding filter (SBF, such as the low-complexity quadrature mirror filter, QMF [13]) before quantization. As an efficient way of parallelization, N-band SBF can directly increase the throughput of temporal ADX by a factor of N, albeit at the cost of additional filtering latency. We found 2-band, 16-tap Johnston QMF to be a good tradeoff between latency and crosstalk (thereby in-band SNR) for SBF. Also, the ADPCM-based quantizer was modified with less-frequent predictor feedback. In total, an entire 61.44MHz ADX throughput was achieved at 122.88MHz clock frequency.

The experimental setup of ADX-RoF transport in a front-haul scenario is depicted in Fig. 1(b). In offline emulation, P independent 5G NR-like OFDM streams were transmitted over P×16 MIMO flat Rayleigh fading channel [9], resulting in 16-channel signals. The signals had a sample rate of 61.44MHz and was 1024QAM-modulated. 3300 out of 4096 subcarriers [14] were used to carry data, and the radio bandwidth is about 50MHz. Cyclic prefix (CP) size is 512. The length of training sequence (TS) for MIMO channel estimation and payload were P and 2 OFDM symbols, respectively. 768-sample preamble was added to assist the convergence of the spatial ADX. After adding noise, the 16 channels were loaded in the RAM of hardware. To emulate in real time the 16-channel radio reception in this MIMO RoF system, we chose the Xilinx RFSoC hardware platform that integrates 16-channel, GHz-bandwidth DAC&ADC array, digital RF chain and FPGA on a single chip. The 16-channel signals in the RAM were up-converted to an intermediate frequency (IF) of 100MHz and emitted by the on-chip 14bit DAC array operating at 983.04MSa/s. The measured spectra of 3 analog IF-OFDM channels among 16 are depicted in inset (ii) of Fig. 1(b), showing about 5~10dB power difference due to the MIMO fading channel.

In remote radio unit (RRU), the on-chip 12bit ADC array digitized these 16 IF channels at 983.04MSa/s, followed by down-conversion to baseband and resampling to 61.44MHz. The real-time ADX performed compression at 61.44MHz throughput, including 16-to-4channel spatial ADX with PAST-based filter update and 8-bit temporal ADX (subband ADPCM). No FIFO was used before ADX, as the throughput is sufficient for the 61.44MHz signals. 112711 LUTs and 1452 DSPs resource were used for implementing the ADX. The compressed bitstream after ADX was 64b/66b line coded [2] and output by the GTY serial transceiver with a resulting bit rate of 4.05504Gb/s. Considering the control word overhead of 16/15 and line coding overhead of 66/64, the CPRI-equivalent rate in this case is 32.4Gb/s = 61.44(MHz)×(15×2)×16×overhead. The compression ratio of ADX compared with CPRI is 4/16×8/15≈13.3%. The electrical OOK output by GTY was amplified and modulated onto an optical carrier at 1552.5nm via a LiNbO3 Mach-Zehnder modulator. The optical OOK signal (~2dBm power) encapsulating radio waveforms was then transmitted over 23.5km single-mode fiber (SMF) to the baseband unit (BBU). A variable optical attenuator (VOA) was used to vary the received optical power. In BBU, the OOK signal was received by a 12.5Gb/s photodetector (PD) and captured by a Tektronix oscilloscope operating at 12.5GSa/s. Offline processing includes down-sampling, OOK bit decision, line decoding, ADX decompression, MIMO demodulation, and EVM evaluation. We didn't use link forward error correction (FEC) or electrical equalizer.

3. Experimental Results and Discussion

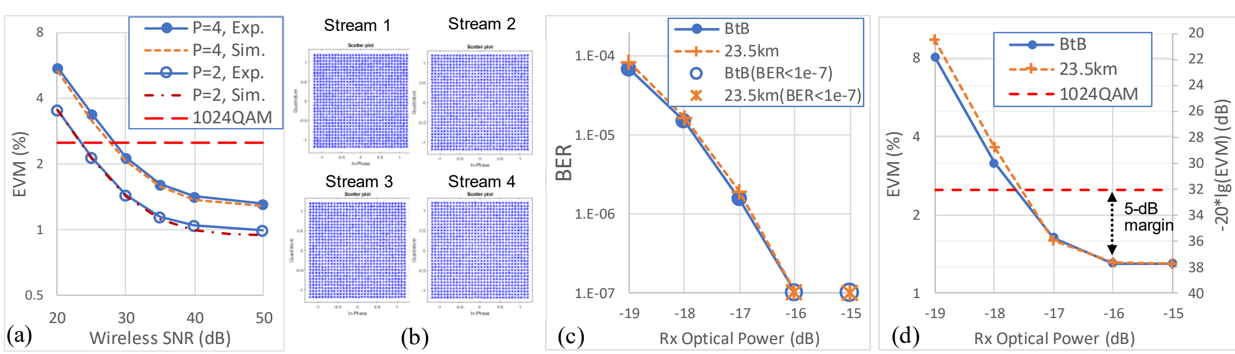

Fig. 2. Experimental results. (a) EVM vs. wireless SNR, along with Matlab simulation results. (b) Constellations of 4 streams (wireless SNR=50dB). (c) Optical link BER vs. Rx optical power. (d) EVM vs. Rx optical power.

First, the performance of real-time ADX with different wireless SNR was evaluated. The fiber link was assumed to be error-free. The EVM versus wireless SNR is shown in Fig. 2(a), where each experimental EVM value is an average of P streams and 10 different MIMO channel realizations. The ADX supported cases of P=1~4, and here we show the cases of P=4 and P=2. In P=4 case, EVM was less than 2.5% or 32dB (threshold for 1024QAM [15]) when wireless SNR was larger than 30dB. The EVM floor, mainly caused by the temporal ADX, was around 1.3% (37.7dB). Fig. 2(b) shows constellations of 4 streams at wireless SNR=50dB. In P=2 case, since the ADX provided more spatial diversity gain [10], EVM was <1% or >40dB when wireless SNR=50dB. Note that throughout this work, TS were also compressed by ADX without being processed separately from payload, which in fact affected the accuracy of MIMO channel estimation. Nevertheless, such high EVM performance was still achieved, highlighting the fidelity of our real-time ADX.

Next, we fixed P=4 and wireless SNR at 50dB, and investigated the impact of fiber link error. Fig. 2(c) shows link BER vs. received optical power of both back-to-back (BtB) case and after 23.5km SMF transmission. After ADX, the line rate became only about 4Gb/s, which led to negligible dispersion-induced penalty. The simple OOK format allows the use of cost-effective optical transceivers in practice. Fig. 2(d) shows measured EVM vs. received optical power. All 4 uplink streams had EVM of less than 1.4% (37dB) when the received optical power was -16dBm or larger, which offered 5dB EVM margin (w.r.t. 1024QAM threshold) for, e.g., practical RF chain. By comparing Fig. 2(c) and 2(d), it was observed that the real-time ADX can tolerate at least 1.95e-6 link BER without exceeding 1024QAM EVM threshold. Thus, one can adopt simple link FEC or even omit FEC as a joint design of wireless (compression) and wired part (channel coding).

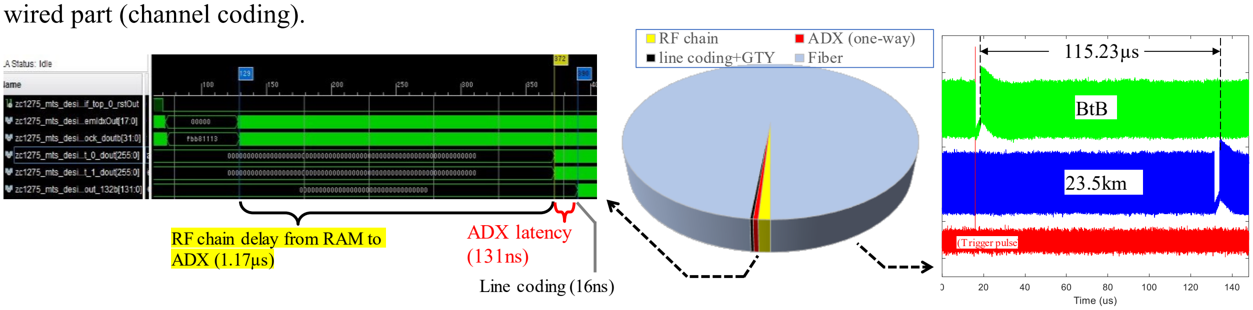

Fig. 3. Experimental results: latency break-down of the demonstrated ADX-RoF link.

Finally, the ADX latency experimentally measured by Vivado Integrated Logic Analyzer (ILA) is shown on the left side of Fig. 3. The ADX had a latency of 131ns (i.e., 16 clock cycles or CC), including 16ns from spatial ADX, 74ns from SBF, 33ns from ADPCM, and 8ns register. Moreover, according to Vivado FPGA simulation, the latency of ADX decompression at BBU is 342ns (i.e., 44 CC). In total, the ADX-induced one-way latency overhead is (131+342)ns<500ns. Fig. 3 also shows latency break-down of the demonstrated ADX-RoF link (except the offline BBU part), including measured RF chain delay (1.17μs), line coding latency (16ns), GTY latency (~260ns), and fiber propagation delay of ~115.23μs as shown by the captured waveforms in optical BtB and 23.5km transmission cases. Indeed, our real-time ADX has negligible latency overhead compared with either fiber propagation delay or 3GPP one-way transport network latency budget of 250μs [16].

4. Conclusion

We have demonstrated MIMO ADX-RoF transport of 16-channel, 1024QAM, 61.44MHz 5G NR-class signals over 23.5km, enabled by the real-time ADX prototyped on a single-chip radio platform. The RoF link provides <1.4% average EVM at a received optical power of -16dBm. <500ns one-way processing latency overhead of the ADX has been achieved.

Acknowledgement: this work was supported by the R&D contract (FY2017~2020) "Wired-and-wireless converged radio access network for massive IoT traffic" for radio resource enhancement by the Ministry of Internal Affairs and Communications, Japan.

5. References

[1] Y. Yoshida, Proc. OFC 2018, Tu2K.1 (Tutorial).
[2] CPRI, "CPRI Specification v7.0," Technical Report, 2015.
[3] M. Xu et al., JLT **35**, 3671-3679 (2017).
[4] H. Jung et al., IEEE PTL **28**, 661-664 (2015).
[5] J. Zhang et al., JLT **35**, 989-996 (2017).
[6] A. Kanno et al., IEEE Photon. J. 4, 2196-2204 (2012).
[7] R. Puerta et al., JLT **36**, 587-593 (2018).
[8] Y. Yoshida et al., Proc. SPIE *Broadband Access Communication Technologies XIII* 2019, p. 109450C.
[9] P. Zhu et al., Proc. ECOC 2019, M1C.2.
[10] P. Zhu et al., Opt. Express **26**, 24098-24113 (2018).
[11] B. Yang, IEEE Trans. Signal Process. **43**, 95-107 (1995).
[12] ITU-T Recommendations G.726.
[13] K. Sayood, *Introduction to data compression* (Newnes, 2012).
[14] 3GPP TS 38.211, V15.3.0, Sept. 2018.
[15] 3GPP TS 36.104, V15.2.0, Mar. 2018.
[16] 3GPP TR 38.801, V14.0.0, Mar. 2017.